8-24-2020

Deciphering the unique structure and acylation pattern of Posidonia oceanica lignin

Jorge Rencoret

Gisela Marques

Oscar Serrano
Edith Cowan University

Joeri Kaal

Angel T. Martínez

See next page for additional authors

10.1021/acssuschemeng.0c03502
Rencoret, J., Marques, G., Serrano, O., Kaal, J., Martínez, A. T., del Río, J. C., & Gutiérrez, A. (2020). Deciphering the unique structure and acylation pattern of Posidonia oceanica lignin. ACS Sustainable Chemistry & Engineering, 8(33), 12521-12533. https://doi.org/10.1021/acssuschemeng.0c03502

ACS Sustainable Chemistry & Engineering

pubs.acs.org/journal/ascecg

Research Article

Deciphering the Unique Structure and Acylation Pattern of *Posidonia oceanica* Lignin

Jorge Rencoret,*,‖ Gisela Marques,‖ Oscar Serrano, Joeri Kaal, Angel T. Martínez, José C. del Río, and Ana Gutiérrez

Cite This: *ACS Sustainable Chem. Eng.* 2020, 8, 12521−12533

Read Online

ACCESS | Metrics & More | Article Recommendations | Supporting Information

ABSTRACT: Lignins from different parts of the seagrass *Posidonia oceanica*—namely sheaths, rhizome, and roots—as well as from fibrous balls from *P. oceanica* detritus were isolated and thoroughly characterized by pyrolysis coupled with gas chromatography/mass spectrometry, derivatization followed by reductive cleavage, two-dimensional nuclear magnetic resonance spectroscopy, and gel permeation chromatography. The lignins of *P. oceanica* were enriched in guaiacyl (G) over syringyl (S) units, with S/G ratios ranging from 0.1 (fibrous balls) to 0.5 (rhizome). $\beta-O-4'$ ethers and phenylcoumarans were the most abundant lignin substructures, followed by resinols, and minor amounts of dibenzodioxocins and spirodienones. Moreover, all lignins were found to be highly γ-acylated (up to 44% of total units), mainly with *p*-hydroxybenzoates but also, to a lesser extent, with acetates. The data indicated that this acylation extensively occurred in both G- and S-lignin units, contrary to what happens in palms, poplar, and willow, where *p*-hydroxybenzoates overwhelmingly appear at the γ-position of S-units.

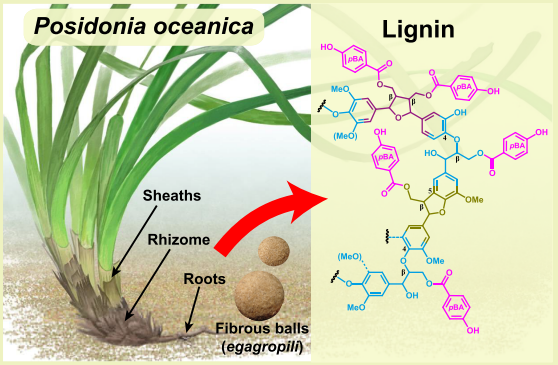

KEYWORDS: *p-Hydroxybenzoates, 2D-NMR experiments, Seagrasses, Recalcitrance, Organic chemistry*

INTRODUCTION

Lignin ranks among the most abundant polymers in the plant kingdom, where it plays a key role as structural component for cell-wall assembly. Because of its recalcitrant nature, lignin contributes approxymately 30% of the annual carbon sequestration potential in plant materials[1] and plays a significant role in terrestrial and oceanic carbon cycles.[2] Traditionally, lignin has been defined as a polymeric structure resulting from the coupling of three monolignols—*p*-coumaryl, coniferyl, and sinapyl alcohols—that give rise to the corresponding *p*-hydroxyphenyl (H), guaiacyl (G), and syringyl (S) phenylpropanoid units.[1,3,4] The composition and structure of this complex polymer do not follow a predetermined pattern but vary significantly among and within plant species, including differences in lignin composition of cell-wall layers, tissues, and organs driven by the age of the plant and environmental conditions.[5−8]

During the last two decades, however, it has been found that many other phenolic compounds beyond the three traditional monolignols can also act as real lignin monomers.[9] For example, monolignol ester conjugates (with acetates, *p*-coumarates, and *p*-hydroxybenzoates and to a lesser extent with ferulates, vanillates, and benzoates) have been found in a variety of plants species.[10−17] These acylated monolignols are fully compatible with lignification reactions, and plants can use them to synthesize γ-acylated lignin. Naturally γ-acetylated monolignols are widespread among angiosperms, with some species containing lignins with high (up to 80%) acetylation degrees.[12,13] *p*-Coumaroylated monolignols are also commonly found in grasses as well as in other monocots,[16,18] whereas *p*-hydroxybenzoylated monolignols are found in palms, willow, and poplar.[14,19,20] Incorporation of these γ-acylated monolignols into the lignin polymer through $\beta-\beta$ coupling leads to the formation of characteristic tetrahydrofuran structures, the presence of which is irrefutable evidence that γ-acylated monolignols act as real lignin monomers.[20−22]

A common feature in all the aforementioned γ-acylated lignins is that the acylating groups are found primarily in the side chain of S-units, with little or negligible acylation taking place on G-units. However, the seagrass *Posidonia oceanica*, an endemic species in the Mediterranean Sea, has a unique lignin acylation pattern, being extensively acylated with *p*-hydroxybenzoic acid (*p*BA) over both G- and S-units.[23,24] *P. oceanica* is an angiosperm monocot from the family Posidoniaceae that, despite growing in marine environments, evolved from

Received: May 11, 2020
Revised: July 16, 2020
Published: July 24, 2020

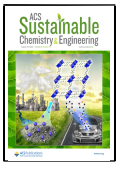

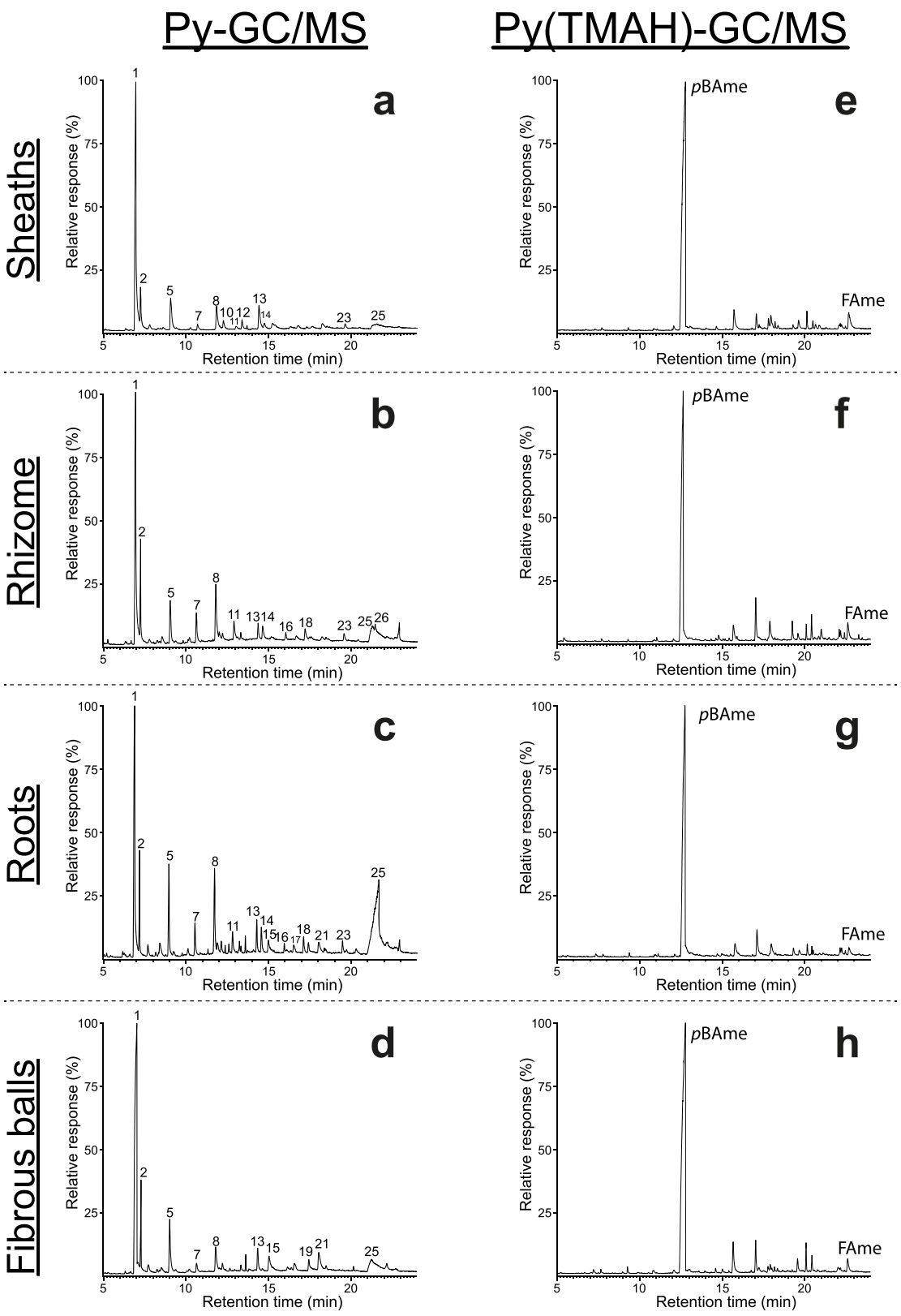

Figure 1. Pyrograms of the MWL preparations from *P. oceanica* sheaths, rhizome, roots and fibrous balls, obtained in absence (a–d) and in the presence of TMAH (e–h). The relative abundances of the identified compounds are detailed in Table 1. In the case of the pyrograms acquired in the presence of TMAH (e–h), only 4-methoxybenzoic acid methyl ester (***p*BAme**) and methyl *trans*-4-methoxyferulate (**FAme**), coming from *p*BA and FA, respectively, are indicated.

terrestrial vascular plants.[25,26] The above finding represents the first exception to the established belief that *p*BA, like acetic and *p*-coumaric acids, selectively acylates S-units and further confirmed the great variability in the composition and structure of lignin within the plant kingdom. Preliminary analysis by the so-called derivatization followed by reductive cleavage

https://dx.doi.org/10.1021/acssuschemeng.0c03502
ACS Sustainable Chem. Eng. 2020, 8, 12521−12533

Table 1. Abundances (Expressed as Percentages of Molar Areas Relative to Total Lignin-Derived Compounds, H+G+S=100) of the Main Phenolic Compounds Identified among the Py-GC/MS Products of MWL Isolated from the Different Parts of the *P. oceanica* Plants and Balls[a]

no.	compound	origin	sheaths	rhizome	roots	balls
1	phenol	*p*BA/H	169.5	112.0	91.2	246.1
2	guaiacol	G	17.8	19.6	14.5	17.3
3	4-methylphenol	H	3.1	1.7	3.5	5.1
4	3-methylphenol	H	2.0	4.0	5.6	4.3
5	4-methylguaiacol	G	19.6	13.7	16.5	23.6
6	4-ethylphenol	H	0.8	0.6	1.3	1.4
7	4-ethylguaiacol	G	2.7	8.3	5.7	3.9
8	4-vinylguaiacol	G/FA	13.2	17.7	16.2	11.8
9	4-vinylphenol	H	1.0	2.6	2.4	1.4
10	eugenol	G	4.0	1.5	2.2	2.2
11	syringol	S	1.6	5.4	4.1	0.3
12	*cis*-isoeugenol	G	3.4	1.1	1.3	1.5
13	*trans*-isoeugenol	G	12.8	3.2	4.7	7.0
14	4-methylsyringol	S	2.9	2.8	4.1	tr
15	vanillin	G	6.7	1.7	3.5	10.8
16	4-ethylsyringol	S	0.2	1.5	1.0	tr
17	acetoguaiacone	G	2.1	1.9	2.1	3.9
18	4-vinylsyringol	S	0.7	3.4	2.8	tr
19	guaiacylacetone	G	1.4	tr	1.9	3.6
20	4-allylsyringol	S	0.4	0.4	0.4	tr
21	4-hydroxybenzoic acid, methyl ester	*p*BA	3.9	1.3	4.2	11.0
22	*cis*-4-propenylsyringol	S	0.4	0.6	0.6	1.1
23	*trans*-4-propenylsyringol	S	1.6	1.8	1.9	tr
24	syringaldehyde	S	0.4	0.5	0.9	0.3
25	4-hydroxybenzoic acid	*p*BA	20.4	34.8	85.5	42.8
26	acetosyringone	S	0.7	3.4	1.6	0.3
27	propiosyringone	S	0.2	0.8	0.5	0.1
28	3-(3,5-dimethoxy-4-hydroxyphenyl)-3-oxopropanal	S	0.2	0.8	0.5	0.2
		H (%)[b]	6.9	8.3	13.2	12.3
		G (%)[b]	82.8	66.9	66.9	85.0
		S (%)[b]	10.2	24.8	19.9	2.6
		S/G ratio	0.12	0.37	0.30	0.03

[a]Abbreviations: H, *p*-hydroxyphenyl units; G, guaiacyl units; S, syringyl units; *p*BA, *p*-hydroxybenzoic acid; FA, ferulic acid; tr, traces. [b]Calculated without using phenol (1), methyl 4-hydroxybenzoate (21), 4-hydroxybenzoic acid (25) resulting from *p*BA moieties, and 4-vinylguaiacol (8) arising from FA moieties.

(DFRC)[27] showed that the lignin of *P. oceanica* seagrass was γ-acylated with *p*BA.[24] However, a detailed understanding of the structural characteristics of *P. oceanica* lignin, such as its distribution of interunit linkages and the type of the lignin units involved in them, still remains unknown.

To gain further knowledge into the structure of the exceptional lignin present in *P. oceanica* seagrass, different parts of the plant—including sheaths, rhizome, and roots—and *P. oceanica* balls, the so-called *egagropili* or Neptune balls, which are mostly formed from *P. oceanica* sheath detritus,[28] were studied. The lignins were isolated and comprehensively characterized on the basis of pyrolysis coupled with gas chromotography (Py-GC/MS), DFRC, two-dimensional nuclear magnetic resonance (2D-NMR), and gel permeation chromatography (GPC) analyses. This study aims to describe the composition and structure of *P. oceanica* lignin, as well as the lignocellulosic residue (*egagropili*) that is widely present throughout the Mediterranean coast,[29] and further valorize its potential use in industrial applications. Moreover, the analysis of the fibrous balls will help to evaluate the effects of degradation processes on the *p*-hydroxybenzoylated lignins.

EXPERIMENTAL SECTION

Materials. *P. oceanica* plants were collected in Portlligat Bay (Girona, Spain), a small embayment located on the Costa Brava in the Mediterranean Sea. In the laboratory, plant parts were manually dissected (sheaths, rhizome, and roots), rinsed with seawater to remove adhered particles, quickly dipped into distilled water to remove surface salt, and oven-dried to a constant weight at 40 °C. In addition, *P. oceanica* fibrous balls were sampled at Portlligat Bay for this study. The fibrous balls are mainly formed from *P. oceanica* sheath detritus, but remains of *P. oceanica* leaves and rhizomes together with other unknown organic detritus and inorganic particles can be found.[30] The *P. oceanica* balls were disaggregated to remove inorganic particles and dipped into distilled water prior to drying at 40 °C.

The *P. oceanica* samples (sheaths, rhizome, roots, and balls) were knife-milled and exhaustively Soxhlet-extracted to remove non-structural component of the plant cell-wall, as previously described.[8] The total lignin content of the extractives and water-soluble free *P. oceanica* samples was estimated as the sum of acid-insoluble (Klason lignin) and acid-soluble lignin, determined following the TAPPI methods T222 om-88 and UM 250, respectively.[31]

Lignin Isolation. The lignins from *P. oceanica* sheaths, rhizome, roots, and balls were isolated and purified according to the Björkman's protocol.[32] To obtain this lignin, known as "milled-wood" lignin (MWL), the extracted samples were ball-milled, extracted with dioxane-

https://dx.doi.org/10.1021/acssuschemeng.0c03502
ACS Sustainable Chem. Eng. 2020, 8, 12521−12533

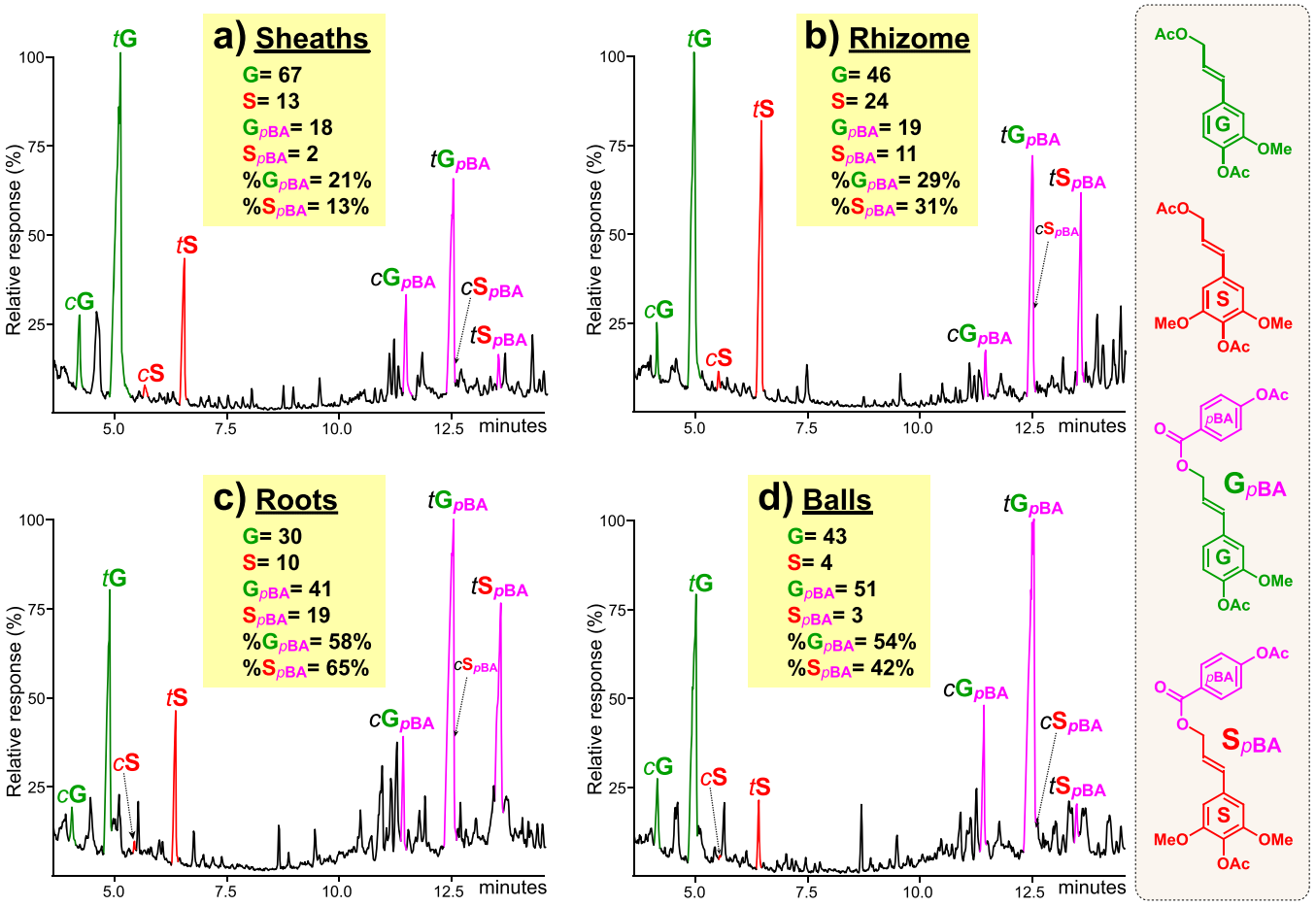

Figure 2. Chromatograms of the DFRC products released from the MWLs of *P. oceanica* sheaths (a), rhizome (b), roots (c), and fibrous balls (d). Boxes indicate the relative abundances of the different γ−OH and γ-*p*BA aromatic units (**G**, **S**, $\mathbf{G}_{pBA}$, and $\mathbf{S}_{pBA}$), totaling 100%, and also the percentages of *p*-hydroxybenzoylated lignin units (%G_{pBA} and %S_{pBA}).

water and then purified, according to the procedure described elsewhere.[33] Final yields of 8−12% referred total lignin contents were obtained.

Analytical Pyrolysis. Lignins isolated from *P. oceanica* samples were pyrolyzed in a Frontier 3030 microfurnace pyrolyzer (Fukushima, Japan), and the phenolic products were analyzed on an Agilent 7820A GC/5975 mass detector (Agilent Technologies, Inc., Santa Clara, CA). More detailed information on pyrolysis experimental conditions can be found in the Supporting Information (SI). The identification of the phenolic compounds released upon pyrolysis was performed by comparison of their mass spectra with those reported in the literature.[14,34] The relative percentages of lignin-derived phenolic compounds were calculated as previously described.[8]

Derivatization Followed by Reductive Cleavage (DFRC). MWL samples (10 mg) were treated according to the original protocols,[27,35] following the detailed procedure described elsewhere.[36] The DFRC products were analyzed and identified by GC/MS, using the equipment and settings described previously.[24] Detailed experimental conditions can be found in the SI.

Lignin Saponification. MWL samples (~30 mg) were dissolved in 5 mL of 1.5 N sodium hydroxide, in a 10 mL reaction vial, and the solution was continuously stirred during 48 h, at 90 °C. After completion, the pH was reduced to 2.0 with 5 N HCl and the solution was stored at 4 °C overnight. Finally, saponified lignin was recovered by vacuum filtration using a 0.45 μm nylon filter, washed with deionized water, and oven-dried at 40 °C.

2D-NMR Analyses. MWL samples (~30 mg) were dissolved in 0.5 mL of deuterated dimethyl sulfoxide (DMSO-d_6) and were analyzed on a Bruker Avance III 500 MHz (Bruker, Karlsruhe, Germany) spectrometer equipped with a cryoprobe. Detailed information about the NMR instrument and the experimental conditions, including experiment types, pulse programs, experimental times, and spectra processing, can be found in the SI.

HSQC correlation peaks were assigned according to the literature[8,14,37] and the quantitation of lignin units and linkages were performed as described elsewhere.[14,37] Details on the signals quantification are found in the SI.

GPC Analyses. For the gel-permeation chromatography analyses, *P. oceanica* lignin samples were acetylated, and then analyzed as previously described (detailed in the SI).[8]

RESULTS AND DISCUSSION

In this work, the lignins present in seagrass *P. oceanica* parts (namely sheaths, rhizome, and roots), as well as the lignin from the *P. oceanica* balls were isolated according to the classical protocol,[32] which allows obtaining practically unaltered lignin, similar to the native lignin.[38] The samples had considerable amounts of lignin, which represented up to 44% of the plant dry weight in balls, 33% in both sheaths and roots, and 31% in rhizome.

Determination of Lignin Composition by Analytical Pyrolysis. The composition of MWL preparations isolated from *P. oceanica* plant parts was first analyzed by Py-GC/MS. The chromatograms of the phenolic compounds released upon pyrolysis of the different MWLs are displayed in Figure 1 (a−d), and the identities of the lignin-derived markers and their relative abundances are detailed in Table 1. In all cases, pyrolysis released phenolic compounds resulting from H-, G-, and S-lignin

https://dx.doi.org/10.1021/acssuschemeng.0c03502
ACS Sustainable Chem. Eng. 2020, 8, 12521−12533

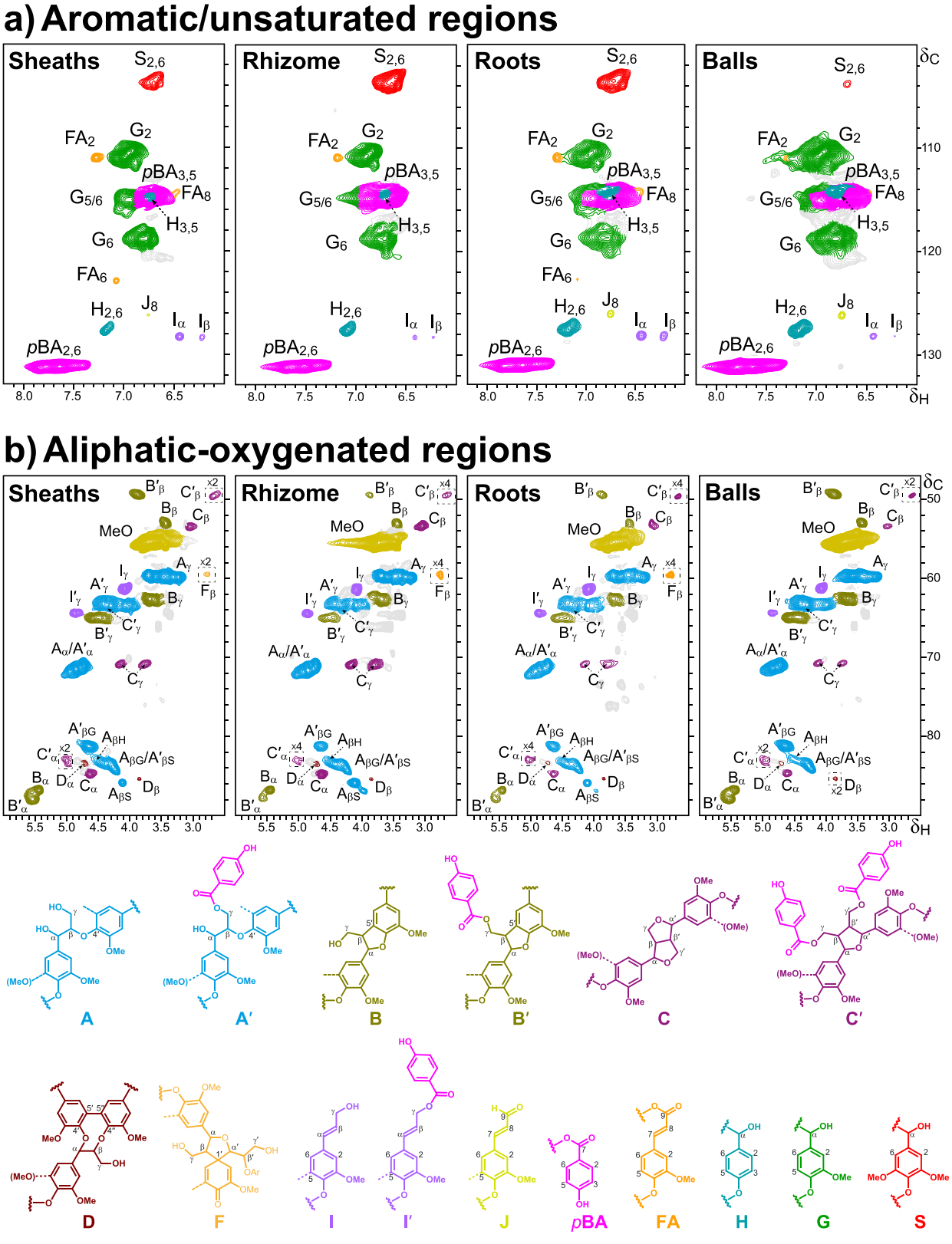

Figure 3. Aromatic/unsaturated (a) and side-chain (b) regions from the HSQC spectra of the isolated lignins from *P. oceanica* sheaths, rhizome, roots and fibrous balls. Lignin structures identified: *β*−*O*−4′ (**A**), *p*BA *γ*-acylated *β*−*O*−4′ (**A′**), *β*−5′ phenylcoumarans (**B**), *p*BA *γ*-acylated phenylcoumarans (**B′**), *β*−*β*′ resinols (**C**), *β*−*β*′ tetrahydrofurans (**C′**), 5−5′ dibenzodioxocins (**D**), *β*−1′ spirodienones (**F**), cinnamyl alcohol terminal-groups (**I**), *p*BA *γ*-acylated cinnamyl alcohol terminal-groups (**I′**), cinnamaldehyde terminal-groups (**J**), *p*-hydroxybenzoic acid moiety (***p*BA**), ferulic acid moiety (**FA**), *p*-hydroxyphenyl units (**H**), guaiacyl units (**G**), and syringyl units (**S**). The structures and contours of the HSQC signals are color coded to aid interpretation. The gray signals in the aliphatic-oxygenated regions correspond mainly to residual carbohydrates. The dashed line boxes indicate sections of the spectrum scaled-up to 2-fold (×2) and 4-fold (×4) intensity.

https://dx.doi.org/10.1021/acssuschemeng.0c03502
ACS Sustainable Chem. Eng. 2020, 8, 12521−12533

units, with phenol (peak 1) being the most abundant (Table 1). However, the unusually high levels of phenol indicate that most of it might not result from H-lignin units, but from the *p*BA groups present in *P. oceanica* lignins that are decarboxylated upon pyrolysis.[24] The pyrolysis data also indicated that lignins were composed primarily of G units, with low S/G ratios for rhizome (0.37), roots (0.30), sheaths (0.12), and fibrous balls (0.03). In order to confirm that phenol arises from *p*BA, pyrolysis was also performed using tetramethylammonium hydroxide (TMAH), which methylates the phenolic and carboxyl groups in the lignin to prevent decarboxylation.[14,39,40] Py(TMAH)-GC/MS chromatograms clearly showed that *p*BA (as its methylated derivative 4-methoxybenzoic acid methyl ester) was by far the most prominent compound released from all lignins (Figure 1e−h), confirming that the phenol released upon pyrolysis did not result from H-lignin units but from the *p*BA moieties, as also observed in other lignins.[8,14,41] In addition, Py(TMAH)-GC/MS analyses also revealed that minor amounts of FA moieties (released as methyl *trans*-4-methoxyferulate) are present in the *P. oceanica* lignins.

Lignin γ-Acylation in *P. oceanica* Seagrass. DFRC, a lignin degradation method designed to cleave β-alkyl-ether linkages, leaving γ-esters intact,[27] provided relevant insights into the nature of the γ-acylation. The *cis/trans* isomers of both guaiacyl (*c*G and *t*G) and syringyl (*c*S and *t*S) units were detected among the DFRC products in all *P. oceanica* lignins analyzed, which resulted from normal lignin units with free γ−OH (Figure 2). However, more interestingly, the DFRC chromatograms also showed important peaks corresponding to the *cis/trans* isomers of *p*BA γ-acylated guaiacyl (cG_{pBA} and tG_{pBA}) and syringyl (cS_{pBA} and tS_{pBA}) lignin units, which conclusively demonstrate that *p*BA are extensively acylating the γ−OH of *P. oceanica* lignins in both G- and S-lignin units. The highest *p*-hydroxybenzoylation degree was found in the lignin from the roots, reaching up to 58% of all G-units and 65% of all S-units (Figure 2). It is important to note that in most plants, as in palms, poplar and willow, *p*-hydroxybenzoylation predominantly occurs on S-units. In the particular case of oil palm empty fruit bunch (EFB), 40% of all S-units were *p*-hydroxybenzoylated, while less than 5% of all G-units were *p*-hydroxybenzoylated.[20] The occurrence of highly *p*-hydroxybenzoylated lignin is not only structurally relevant but also has important implications in terms of lignin biosynthesis because it means that the *p*-hydroxybenzoyl-CoA monolignol transferase involved in their biosynthesis presents high affinities for both coniferyl and sinapyl alcohols.[20,42] No traces of ferulate-monolignol conjugates were found among the DFRC products, indicating that the ferulate moieties detected upon Py/TMAH are not from ferulates attached to the γ−OH as observed in other plants[15] but from ferulates involved in lignin carbohydrate bridges and intrinsically incorporated into the lignin structure.

Furthermore, the occurrence of native acetates that might also occur acylating the γ−OH was assessed by the so-called modified DFRC (DFRC′), that uses propionylating reagents instead of acetylating ones.[35] DFRC′ analysis indicated that acetates were also present as γ-acylating group in all lignins, and principally in the *P. oceanica* sheaths lignin (accounting for 0.2% of all G-units, and 8% of all S-units), and at lower extents in the lignins from rhizome (0.1% of all G-units, and 1.6% of all S-units), roots (0.4% of all G-units, and 2.4% of all S-units), and fibrous balls (less than 0.1% of all G units, and 1.7% of all S-units). Therefore, altogether, the DFRC and DFRC′ analyses indicate that *p*BA is the most important γ-acylating group in these lignins. It is important to note that while lignin acylation with *p*BA does not follow an established pattern in *P. oceanica*, acylation with acetates preferably occur on the side chain of S-units, as is seen in other naturally acetylated lignins. This implies that the acetyl-CoA monolignol transferase involved in their biosynthesis in *P. oceanica* presents more affinity for sinapyl alcohol than for coniferyl alcohol, in contrast to what occurs with the *p*-hydroxybenzoyl-CoA monolignol transferase in *P. oceanica*, that present similar affinities for both sinapyl and coniferyl alcohols.

Lignin Aromatic Units and Bonds as Shown by NMR. The MWLs from *P. oceanica* plant parts were meticulously characterized by a combination of HSQC, HMBC, and HSQC-TOCSY 2D-NMR analyses, as detailed below. The HSQC spectra of *P. oceanica* MWLs, as well as the main lignin structures identified, are shown in Figure 3, and the signals assigned therein, together with their corresponding shifts, are detailed in Table S1. The spectra displayed very well-resolved lignin signals, with some small signals for residual carbohydrates, indicating the suitability of the isolation process.

The HSQC aromatic/unsaturated regions provided detailed insights into the composition of lignins from different parts of the *P. oceanica* plants and balls in terms of aromatic structural units (Figure 3a). In this region, the main correlation signals belonged to **H**, **G** and **S** aromatic units, together with strong signals from ***p*BA** moieties. Signals from **FA** moieties, terminal cinnamyl alcohols (**I**), and cinnamaldehydes (**J**), were also found in the aromatic/unsaturated region. However, it is interesting to note that tricin, a flavone that has been widely found into the lignins from all grasses and other monocots,[43] was not detected in any of the lignins from *P. oceanica* (tricin was also absent in the lignin from the related species *P. australis*, data not shown here). In addition, *p*-coumarates, which are a typical feature of grass lignins,[16] were also absent in *P. oceanica* lignins. The absence of tricin and *p*-coumarates agrees with the fact that the so-called seagrasses are phylogenetically distant from terrestrial grasses being, respectively, classified in the orders Alismatales and Poales.

The HSQC aliphatic-oxygenated regions of isolated MWLs from the *P. oceanica* plant parts and balls (Figure 3b) provided valuable information on how the lignin units are interconnected to each other. The most intense correlation signals, after those of methoxyl groups in lignin units, corresponded to β−*O*−4′ ethers (**A**/**A′**), β−5′ phenylcoumarans (**B**/**B′**), β−β′ resinols/tetrahydrofurans (**C**/**C′**), 5−5′ dibenzodioxocins (**D**), β−1′ spirodienones (**F**), and terminal cinnamyl alcohols (**I**/**I′**).

Among the above linkage signals, those from β−*O*−4′ ethers were the most intense, and two different types of β−*O*−4′ substructures were clearly identified, depending on whether the γ−OH was free ($\mathbf{A}_\gamma$ at δ_C/δ_H 59.7/3.23, 3.58) or acylated by *p*BA ($\mathbf{A'}_\gamma$ at δ_C/δ_H 63.3/4.42, 4.18), as will be shown below. The C_α/H_α signals in both types of substructures ($\mathbf{A}_\alpha/\mathbf{A'}_\alpha$) were overlapped at δ_C/δ_H 71.3/4.79, whereas the C_β/H_β signals in nonacylated β−*O*−4′ substructures connected to a S unit were detected at δ_C/δ_H 85.9/4.12 ($\mathbf{A}_{\beta S}$). However, this signal moved to δ_C/δ_H 83.0/4.33 in γ-acylated β−*O*−4′ substructures ($\mathbf{A'}_{\beta S}$), overlapping with the C_β/H_β signals of nonacylated β−*O*−4′ substructures connected to a G or H unit, which appeared at δ_C/δ_H 83.9/4.27 and 83.3/4.42, respectively. The C_β/H_β signals of γ-acylated β−*O*−4′ substructures connected to a G unit ($\mathbf{A'}_{\beta G}$), which appeared at δ_C/δ_H 81.2/4.65, were distinctly detected in all the MWLs isolated from *P. oceanica*.

https://dx.doi.org/10.1021/acssuschemeng.0c03502
ACS Sustainable Chem. Eng. 2020, 8, 12521−12533

Table 2. 2D-HSQC NMR Semiquantitative Analysis of the Lignin Bonds, Terminal-Groups, γ-Acylation Degree, Structural Units, and FA and *p*BA Moieties in the MWLs Isolated from *P. oceanica* Plant Parts and Balls

	sheaths	rhizome	roots	balls
linkages (%)[a]				
β−*O*−4′ alkyl aryl ethers (**A**/**A**′)	65	74	76	66
β−5′ phenylcoumarans (**B**/**B**′)	25	16	17	27
β−*β*′ resinols (**C**)	5	6	3	4
β−*β*′ tetrahydrofurans (**C**′)	1	1	1	1
5−5′ dibenzodioxocins (**D**)	3	3	3	2
β−1′ spirodienones (**F**)	1	1	1	-
end-groups (%)[a]				
cinnamyl alcohol end-groups (**I**/**I**′)	31	30	35	20
cinnamaldehyde end-groups (**J**)	7	3	6	6
***γ*-acylation degree**				
A′ (% of **A**+**A**′)	43	31	43	42
B′ (% of **B**+**B**′)	58	36	46	66
C′ (% of **C**+**C**′)	27	4	12	28
I′ (% of **I**+**I**′)	33	34	31	30
total average (%)[b]	42	31	41	44
aromatic units				
H (%)	7	9	11	8
G (%)	81	61	68	87
S (%)	13	30	21	5
S/**G** ratio	0.2	0.5	0.3	0.1
ferulates (**FA**, %)[c]	7	5	5	3
p-**hydroxybenzoates** (*p***BA**, %)[c]	83	59	91	90

[a]Estimated as a percentage of the total linkages (**A**−**F**) [b]Calculated considering the abundance and the γ-acylation degree of each structure. [c]FA and *p*BA contents as percentages of lignin content (**H**+**G**+**S**=100).

Phenylcoumaran substructures were also found with the γ−OH free (**B**) or acylated (**B**′). The HSQC spectra displayed two distinguished signals for the each C_α/H_α, C_β/H_β and C_γ/H_γ correlation depending on whether phenylcoumarans were γ-acylated ($\mathbf{B}'_\alpha$, $\mathbf{B}'_\beta$ and $\mathbf{B}'_\gamma$) or not ($\mathbf{B}_\alpha$, $\mathbf{B}_\beta$ and $\mathbf{B}_\gamma$). In the case of *β*−*β*′ linkages, two different types of substructures were identified, resinols (**C**), and tetrahydrofurans (**C**′). The latter can only be formed by oxidative coupling of two previously *p*BA γ-acylated monolignols,[20,21] and, therefore, the presence of this type of structure in *P. oceanica* lignins is a conclusive proof that *p*-hydroxybenzoylation occurs at monolignol level.[20] Signals from dibenzodioxocins (**D**) and spirodienones (**F**) were also observed in all *P. oceanica* lignins, although with lower intensities. Finally, C_γ/H_γ correlation signals corresponding to terminal cinnamyl alcohols (**I**) and its *p*BA γ-acylated analogue (**I**′) were clearly detected.

Semiquantitative Analysis of Lignin Units, Linkages, End-Groups, and Acylation Degree. Semiquantitative analysis of the above HSQC spectra (Table 2), based on signal volume integration, revealed differences in the relative abundances of typical lignin structural units (H, G, and S) and *p*BA and FA moieties, linkages, terminal-groups, and degree of acylation, among the lignins isolated from *P. oceanica* plant parts and balls. H-units accounted from 7% of the total lignin units in the sheath lignin to 11% in the root lignin. G-units were the most abundant ones in all the lignins analyzed, ranging from 61% in rhizomes to 87% in fibrous balls. On the contrary, S-units were more abundant in rhizomes (30%), whereas a minor amount (5%) was found in the lignin of fibrous balls. Taking into account that these balls are largely generated from decayed sheaths, it could be supposed that the original S-units in the lignin of living sheaths are preferentially removed over the G-units, most probably by microbial degradation. The S/G ratios determined by 2D-HSQC spectroscopy in rhizome (0.5), roots (0.3), sheaths (0.2), and fibrous balls (0.1) were in close agreement with those estimated by Py-GC/MS. Regarding the *p*BA moieties, they were more abundant in *P. oceanica* roots lignin, representing up to 91% of the total lignin units (H+G+S = 100), whereas rhizome lignin contained lower amounts of *p*BA moieties (59%). It is important to note that *p*BAs, as will be shown below, are pendant groups attached to the lignin polymer, and consequently, their HSQC correlation signals might be overestimated because of their higher mobility compared with (internal) lignin units (H, G and S).

With respect to the interunit linkages, *β*−*O*−4′ ethers were the most abundant ones in all the *P. oceanica* lignins, ranging from 76% of total linkages in root to 65% in sheaths. Phenylcoumarans were the second most abundant ones and ranged from 27% in balls to 16% in rhizome, whereas resinols/tetrahydrofurans, dibenzodioxocins, and spirodienones were present in smaller proportions in all the lignins (<7%). With regards to lignin end-groups, cinnamyl alcohols were present in considerable amounts, accounting from 20% (referred to total lignin interunit linkages) in the *P. oceanica* balls to 35% in roots, while cinnamaldehyde end-groups were less abundant and only represented 3−7% (Table 2).

The extents of γ-acylation in *β*−*O*−4′ ethers (**A**′), phenylcoumarans (**B**′), tetrahydrofurans (**C**′), and cinnamyl terminal-groups (**I**′) were estimated by integration of C_γ/H_γ HSQC signals corresponding to the free versus acylated γ−OH in each structure. The total and individual percentages of γ-acylation, for each particular lignin substructure, are detailed in Table 2. In general, the data showed that the different *P. oceanica* lignins are extensively γ-acylated, with acylation degrees ranging from 44% in balls to 31% in rhizome. Furthermore, the γ-acylation degree also varied among the different lignin structures. Hence,

https://dx.doi.org/10.1021/acssuschemeng.0c03502
ACS Sustainable Chem. Eng. 2020, 8, 12521−12533

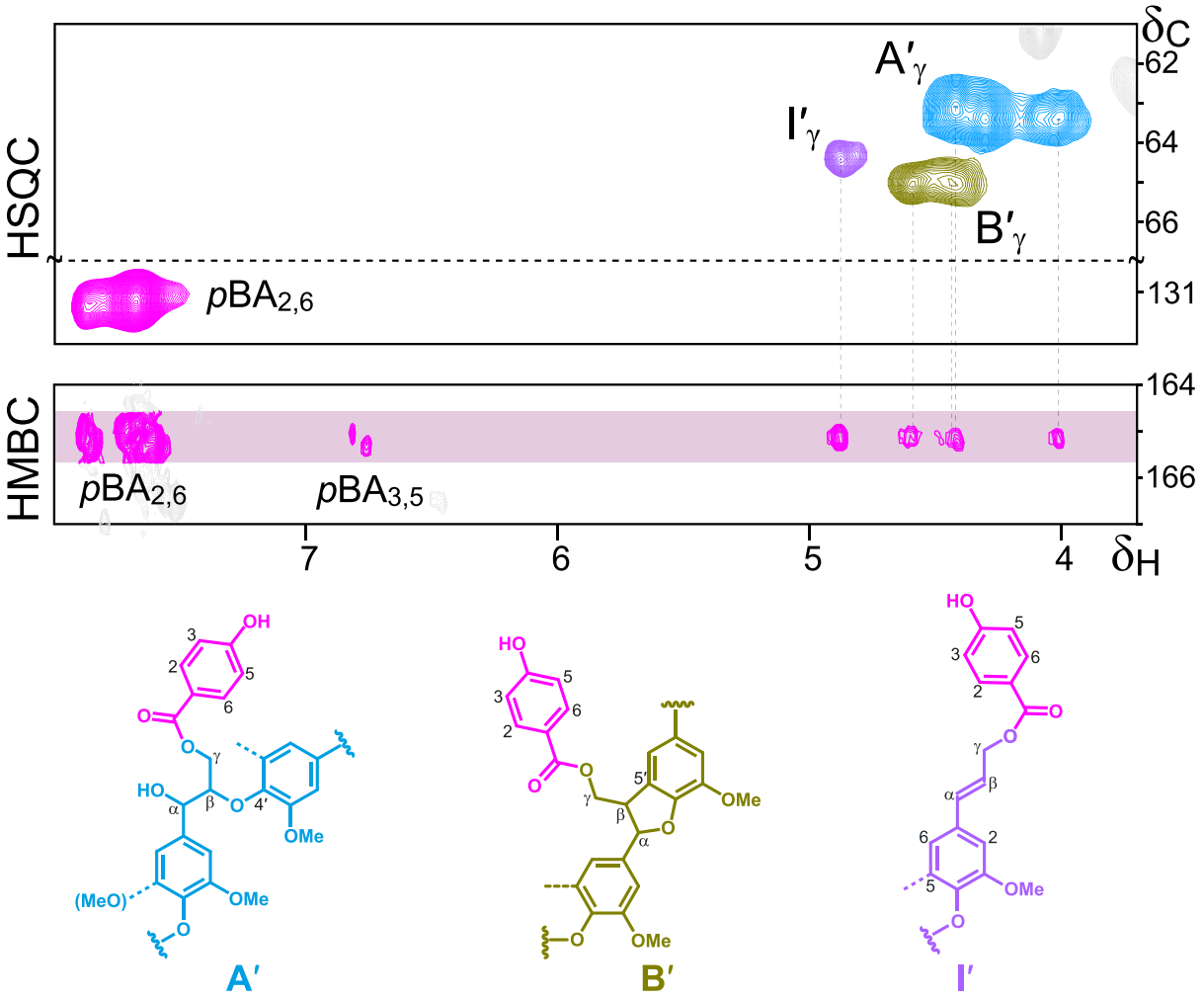

Figure 4. Selected regions of the HMBC and HSQC spectra of *P. oceanica* sheaths MWL that show the correlation of the carboxyl carbon of *p*BA acylating the γ−OH of the lignin side-chains ($\delta_C \sim 165$) in β−*O*−4′ ethers (**A′**), phenylcoumarans (**B′**) and cinnamyl alcohol end-groups (**I′**). Specific regions of the HSQC spectrum displaying the C_γ/H_γ signals of γ-acylated structures (δ_C 61−67) and the $C_{2,6}/H_{2,6}$ signal corresponding to *p*-hydroxybenzoates ($\delta_C \sim 131$) are shown.

phenylcoumarans (**B′**) presented the highest percentage of γ-acylation (36−66%), followed by β−*O*−4′ ethers (**A′**; 31−43%), cinnamyl alcohol terminal-groups (**I′**; 30−34%) and tetrahydrofurans (**C′**; 4−28%). The observed variation in the γ-acylation degree of the different linkage types (β−5′ > β−*O*−4′ > β−β′) could be explained, at least partly, by a slightly higher preferential *p*BA acylation on G units, as β−5′ linkages require more G units to be formed (at least one per structure), while β−*O*−4′ ethers can be formed by both S- or G-units, and most of the β−β′ linkages in angiosperms comprised two S-units.[7] Another reason behind this variation could be related to the differences in the reactivities of γ-*p*BA and γ−OH monolignols for coupling through the different linkages.

Lignin Side-Chain and Ring Connectivities as Shown by HMBC and HSQC-TOCSY. HMBC and HSQC-TOCSY NMR experiments gave complementary data to confirm the signal assignments in the HSQC spectra. The considerable extent of γ-acylation, along with the high amounts of *p*BA detected, suggested that *p*BA are the groups acylating *P. oceanica* lignins, as has also been observed in the lignins from other plants.[8,14,20] To certainly demonstrate that *p*BA moieties act as γ-acylating groups in *P. oceanica* lignins, we used HMBC experiments that display correlation signals between protons and carbons separated by 2−3 bonds. Similar experiments were already used to demonstrate γ-acylation in other lignins.[8,14,22,36,44,45]

The *P. oceanica* lignins presented similar HMBC spectra. Figure 4 displays a selected region of the HMBC spectrum of sheath lignin showing the main correlations for the carboxyl carbons of γ-acylating groups attached to the lignin side-chains. The correlations between the carboxyl carbon at δ_C 165.2 (magenta band) and the protons 2/6 at δ_H 7.65 certified that they belong to the *p*BA moiety. Moreover, this carboxyl carbon also correlates with γ-protons of γ-acylated β−*O*−4′ ethers (**A′**), phenylcoumarans (**B′**), and cinnamyl alcohol terminal-groups (**I′**), which appear in the δ_H range from 4.0 to 5.0, definitively demonstrating that *p*BA are acylating the γ−OH in the different lignins. HMBC correlation signals of *p*BA carboxyl carbon with γ-protons of γ-acylated β−β′ tetrahydrofurans (**C′** in Figure 3) were not detected, most likely because of its low abundance (less than 1.5% of total lignin substructures). A small signal for the carboxyl carbon of acetates could also be detected in the HMBC spectrum (at δ_C 169.9, not shown), although at very low intensity, which is in agreement with the tiny signals of acetates detected in HSQC spectra at $\delta_H/\delta_C \sim 1.9–2.0/20.2$ (not shown) and also confirms the DFRC′ data shown above.

https://dx.doi.org/10.1021/acssuschemeng.0c03502
ACS Sustainable Chem. Eng. 2020, 8, 12521−12533

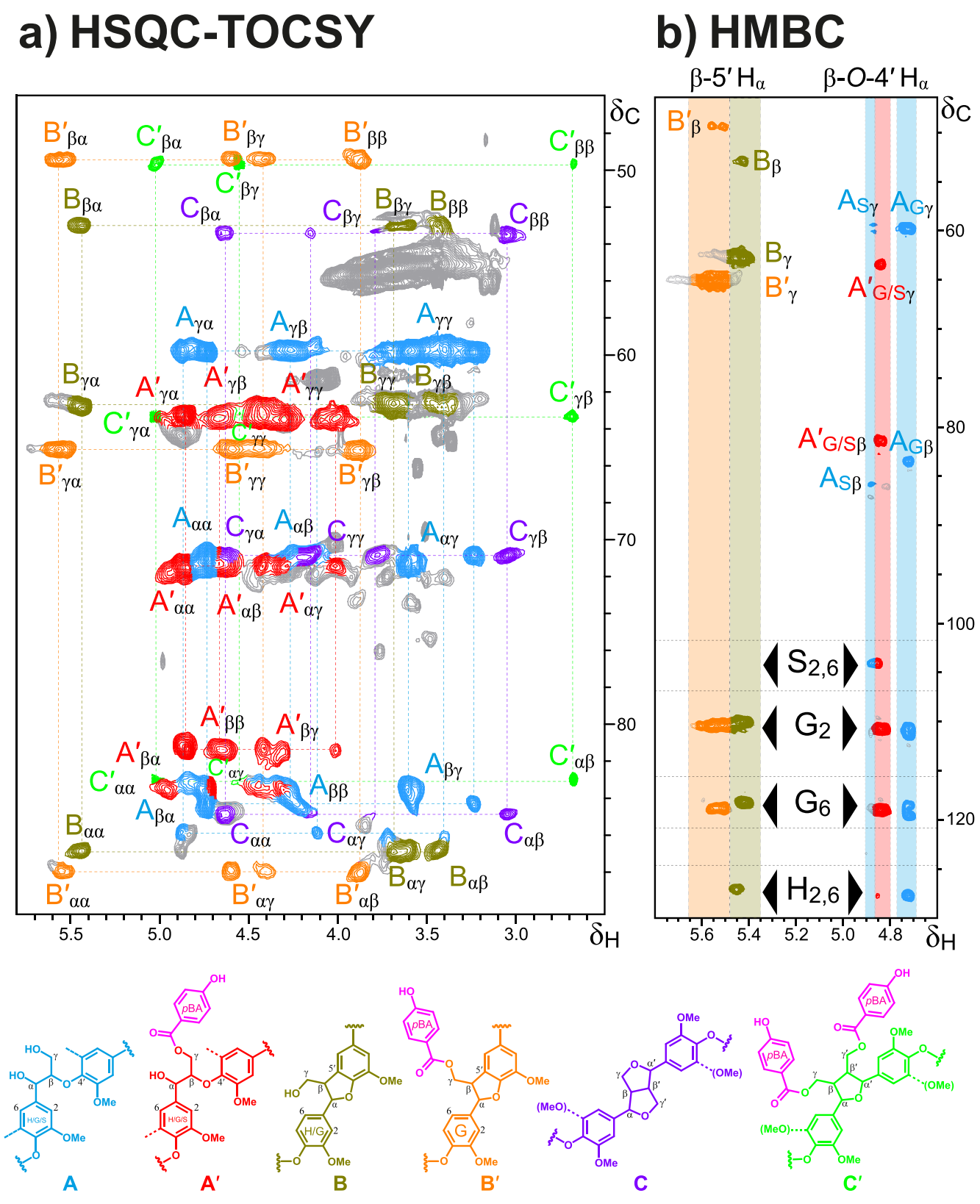

Figure 5. (a) Selected region of the HSQC-TOCSY spectrum of *P. oceanica* sheaths MWL that displays the main cross-signals of the side-chains in *β*−*O*−4′ ethers (**A**/**A**′), phenylcoumarans (**B**/**B**′), and resinol (**C**)/tetrahydrofuran (**C**′) substructures (including both nonacylated and *p*BA *γ*-acylated). (b) Appropriate long-range HMBC spectrum revealing the type of lignin units involved in *β*−*O*−4′ and *β*−5′ bonds. Contour colors matched that of the lignin substructures depicted at bottom. Note that the intensities of HSQC-TOCSY correlation signals corresponding to *p*-hydroxybenzoylated tetrahydrofuran structures (**C**′, in green color) have been augmented to be observed.

The HSQC-TOCSY spectra of the lignins (Figure 5a) were useful to confirm the signal assignments in the HSQC spectra, especially those signals that overlapped with others. The spectra were especially useful to distinguish and assign the signals of the

https://dx.doi.org/10.1021/acssuschemeng.0c03502
ACS Sustainable Chem. Eng. 2020, 8, 12521−12533

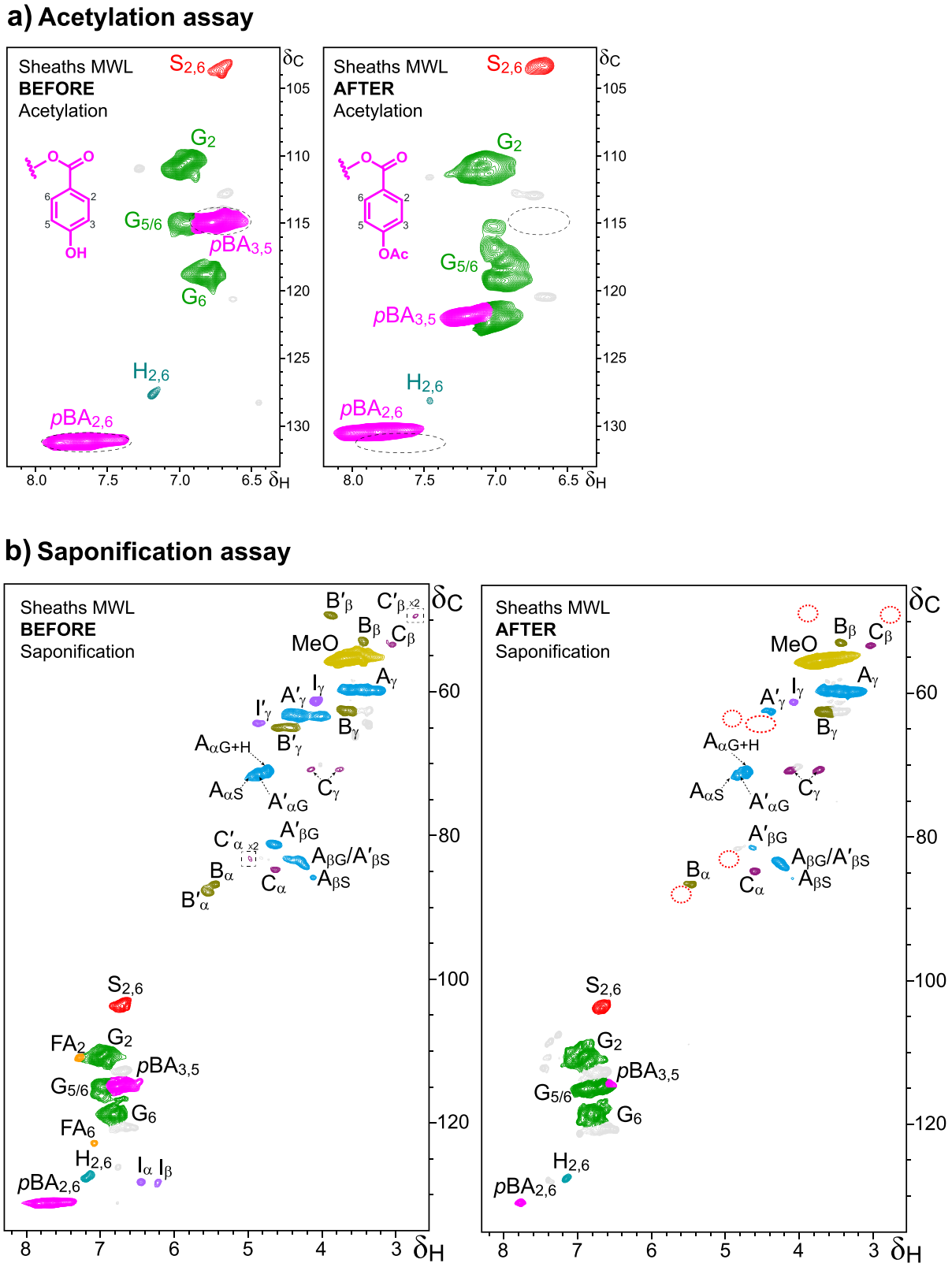

Figure 6. (a) HSQC spectra of *P. oceanica* sheaths MWL, prior and after *in vitro* acetylation, showing that *p*BA correlation signals (especially $pBA_{3,5}$) are shifted after acetylation and, therefore, confirming that all 4-OH in *p*BA are free (susceptible to be acetylated) in the native *P. oceanica* lignins. (b) HSQC spectra of *P. oceanica* sheaths MWL, prior and after saponification with 1.5 M NaOH, reveling that the vast majority of *p*BA are removed after chemical hydrolysis and only a minor amount of *p*BA remains acylating *β*−*O*−4′ structures.

side chains (C_α/H_α, C_β/H_β, and C_γ/H_γ) in the *p*BA *γ*-acylated substructures (**A**′, **B**′, and **C**′), as shown in Figure 5a for the lignin of *P. oceanica* sheaths. On the other hand, Figure 5b shows a selected region of the HMBC spectrum of *P. oceanica* sheath lignin, displaying long-range $^1H/^{13}C$ correlations of H_α in *β*−*O*−4′ ethers (**A**/**A**′) and phenylcoumarans (**B**/**B**′), and

https://dx.doi.org/10.1021/acssuschemeng.0c03502
ACS Sustainable Chem. Eng. 2020, 8, 12521−12533

provides valuable information on which types of lignin unit (H, G, or S) participate in the formation of these major lignin substructures. The HMBC spectrum revealed that *p*BA γ-acylated H-, G-, and S-lignin units are involved in β−*O*−4′ alkyl-aryl ether structures, whereas *p*BA γ-acylated phenylcoumaran structures are formed exclusively by G-units. This fact is of particular relevance because it calls into question the suitability of the DFRC method for the precise determination of *p*BA γ-acylated units in *P. oceanica* lignins. It is known that β−5′ linkages are resistant to DFRC conditions, and consequently, lignin monomers involved in this type of substructure are not released.[27,46] Therefore, DFRC analysis of *P. oceanica* lignins underestimates the real amounts of *p*BA γ-acylated G-units. The absence of S-lignin units in *p*BA γ-acylated β−5′ structures revealed by the HMBC spectra fully agrees with the absence, in the HSQC spectra, of the characteristic $B'_{\alpha S}$ signal corresponding to *p*BA γ-acylated S−G phenylcoumaran structures, which should appear at δ_H/δ_C88.6/5.71.[8] Finally, HMBC spectra also revealed that H-lignin units involved in β−*O*−4′ and β−5′ linkages were largely non-γ-acylated, especially in the latter.

NMR Evidence of *p*BA as Pending Group in *P. oceanica* Lignins. Although the HSQC, HMBC, and HSQC-TOCSY data already seemed to indicate that *p*BA in *P. oceanica* lignins was present as pending (terminal) free-phenolic ester, this was further demonstrated by analyzing the lignins after *in vitro* acetylation. The HSQC spectrum of the acetylated lignins (Figure 6a) clearly showed how $pBA_{2,6}$ and $pBA_{3,5}$ signals, especially the latter, shifted after acetylation. This shifting can only be explained if the *p*BA phenolic OH-group becomes acetylated, which means that *p*BA occurs as free-phenolic ester in native *P. oceanica* lignin, as also occurs in the lignin of other monocots.[8,14,20,47]

To corroborate the above finding, *P. oceanica* lignins were further submitted to mild saponification reactions, which hydrolyze ester bonds but maintains ether and carbon−carbon linkages. The HSQC spectra of the saponified lignins clearly showed that the lignin backbone structure remained intact while terminal *p*BA groups were largely hydrolyzed and cleaved, as shown in Figure 6b for the sheath lignin. Only a very small fraction of *p*BA resisted saponification, those acylating the γ−OH in β−*O*−4′ substructures, as can be deduced by the presence of their characteristic A'_{β} and A'_{γ} signals. In contrast, the characteristic signals of *p*BA γ-acylated phenylcoumarans (B'_{α}, B'_{β}, and B'_{γ}) and tetrahydrofurans (C'_{α} and C'_{β}) substructures and terminal cinnamyl alcohols (I'_{γ}) were totally removed, and only cross-signals of nonacylated phenylcoumarans, resinols, and terminal cinnamyl alcohols were detected in the spectra of the saponified lignins.

GPC Analyses of *P. oceanica* Lignins. GPC chromatograms of the MWLs isolated from *P. oceanica* samples (Figure S1) revealed that the different lignins presented comparable values of the molecular weight-average molecular weight (6450−6100 g mol^{-1}) and number-average molecular weight (3320−2740 g mol^{-1}) and therefore exhibited relatively low polydispersity indexes (1.9−2.2), as indicated in Table 3. These GPC data are comparable to other isolated lignins,[8] and rule out the presence of low molecular weight aromatic structures, including dimers, trimers, or tetramers, in these MWL preparations. This fact is significant because *P. oceanica* seagrass also contains nonstructural *p*BA γ-acylated neolignans,[48] whose presence could have interfered with the chemical characterization of the polymeric lignin. The GPC data were, therefore, useful to confirm that these neolignans were entirely removed from *P. oceanica* samples during Soxhlet extraction prior to lignin isolation.

Table 3. Weight-Average Molecular Weight (M_w), Number-Average Molecular Weight (M_n), and Polydispersity Index (PDI = M_w/M_n) of the MWLs Isolated from the *P. oceanica* Plant Parts and Balls

	sheaths	rhizome	roots	balls
M_w	6390	6300	6450	6100
M_n	3100	2950	3320	2740
PDI (M_w/M_n)	2.1	2.1	1.9	2.2

CONCLUSIONS

The structure of the lignins isolated from *P. oceanica* plant parts and the fibrous balls has been thoroughly studied by cutting-edge techniques in the analysis of lignin, such as 2D-NMR, DFRC, Py(TMAH)-GC/MS, Py-GC/MS, and GPC. The analyses revealed variations in the composition and structure of lignin among different anatomical parts in the same plant and changes during decay and that its structure does not follow a specific acylation pattern. *P. oceanica* lignins were found to be composed mainly of G units, and highly γ-acylated by *p*BA. 2D-NMR analysis also revealed the existence of significant amounts of *p*BA γ-acylated G-units involved in phenylcoumaran structures that are undetectable by DFRC, the method most commonly used to determine the γ-acylation degree in lignin. In addition, 2D-NMR data showed that the *p*-hydroxybenzoylated G-, S-, and H-units are completely integrated into the lignin structure. In this sense, lignin in other plants (such as poplar) could be genetically modified to incorporate higher amounts of *p*BA by expressing the gene of the *p*-hydroxybenzoyl-CoA monolignol transferase involved in the biosynthesis of *p*-hydroxybenzoylated monolignols in *P. oceanica*. On the other hand, it was found that the lignin in *P. oceanica* balls, a very abundant seagrass residue throughout the Mediterranean coast, is highly enriched in *p*BA esters and, therefore, could be an interesting feedstock to produce value-added products for cosmetic and pharmaceutical industries. The particularly high *p*-hydroxybenzoylation levels present in *P. oceanica* lignin can provide an alternative and interesting source of *p*-hydroxybenzoic acid for synthesizing chemicals (parabens) or pharmaceuticals (paracetamol) that are nowadays produced from fossil resources.[49]

ASSOCIATED CONTENT

Supporting Information

The Supporting Information is available free of charge at https://pubs.acs.org/doi/10.1021/acssuschemeng.0c03502.

GPC chromatograms of the MWLs isolated from *P. oceanica* samples, assignments of $^{13}C/^{1}H$ correlation signals in the HSQC spectra of the lignins from *P. oceanica* and detailed experimental conditions for pyrolysis, DFRC, 2D-NMR, and GPC analyses (PDF)

AUTHOR INFORMATION

Corresponding Author

Jorge Rencoret − *Instituto de Recursos Naturales y Agrobiología de Sevilla, CSIC, E-41012 Seville, Spain;* orcid.org/0000-0003-2728-7331; Email: jrencoret@irnase.csic.es

https://dx.doi.org/10.1021/acssuschemeng.0c03502
ACS Sustainable Chem. Eng. 2020, 8, 12521−12533

Authors

Gisela Marques − *Instituto de Recursos Naturales y Agrobiología de Sevilla, CSIC, E-41012 Seville, Spain*

Oscar Serrano − *School of Science, Centre for Marine Ecosystems Research, Edith Cowan University, 6027 Perth, Western Australia, Australia*

Joeri Kaal − *Institut fur Geo-Ökologie, Abt. Umweltgeochemie, Technische Universität Braunschweig, 38106 Braunschweig, Germany*

Angel T. Martínez − *Centro de Investigaciones Biológicas Margarita Salas, CSIC, E-28040 Madrid, Spain;* orcid.org/0000-0002-1584-2863

José C. del Río − *Instituto de Recursos Naturales y Agrobiología de Sevilla, CSIC, E-41012 Seville, Spain;* orcid.org/0000-0002-3040-6787

Ana Gutiérrez − *Instituto de Recursos Naturales y Agrobiología de Sevilla, CSIC, E-41012 Seville, Spain;* orcid.org/0000-0002-8823-9029

Complete contact information is available at: https://pubs.acs.org/10.1021/acssuschemeng.0c03502

Author Contributions

[‖]J.R., G.M.: These authors contributed equally to this work. J.R. designed the study and, together with G.M., performed the experimental work. OS collected the *P. oceanica* samples. J.R., J.C.R., A.T.M., J.K., O.S., and A.G. wrote the manuscript, and the final version was approved by all the authors.

Funding

This work was financed by the Spanish projects AGL2017-83036-R and BIO2017-86559-R, and the CSIC projects PIE-201620E081 and PIE-201740E071. OS was funded by an ARC DECRA DE170101524 and JK by the Deutsche Forschungsgemeinschaft (DFG) project BI 734/18-1.

Notes

The authors declare no competing financial interest.

■ ACKNOWLEDGMENTS

We thank Dr. Manuel Angulo from SGI-CITIUS for acquiring all the NMR spectra presented in this work and also Toni Llobet for his support in preparing the TOC.

■ REFERENCES

(1) Boerjan, W.; Ralph, J.; Baucher, M. Lignin biosynthesis. *Annu. Rev. Plant Biol.* **2003**, *54* (1), 519−546.

(2) Opsahl, S.; Benner, R. Distribution and cycling of terrigenous dissolved organic matter in the ocean. *Nature* **1997**, *386*, 480−482.

(3) Ralph, J.; Lundquist, K.; Brunow, G.; Lu, F.; Kim, H.; Schatz, P. F.; Marita, J. M.; Hatfield, R. D.; Ralph, S. A.; Christensen, J. H.; Boerjan, W. Lignins: Natural polymers from oxidative coupling of 4-hydroxyphenyl- propanoids. *Phytochem. Rev.* **2004**, *3* (1−2), 29−60.

(4) Vanholme, R.; Demedts, B.; Morreel, K.; Ralph, J.; Boerjan, W. Lignin biosynthesis and structure. *Plant Physiol.* **2010**, *153* (3), 895−905.

(5) Campbell, M. M.; Sederoff, R. R. Variation in lignin content and composition: Mechanisms of control and implications for the genetic improvement of plants. *Plant Physiol.* **1996**, *110* (1), 3−13.

(6) Lourenço, A.; Rencoret, J.; Chemetova, C.; Gominho, J.; Gutiérrez, A.; del Río, J. C.; Pereira, H. Lignin composition and structure differs between xylem, phloem and phellem in *Quercus suber* L. *Front. Plant Sci.* **2016**, *7*, 1612.

(7) Rencoret, J.; Gutiérrez, A.; Nieto, L.; Jiménez-Barbero, J.; Faulds, C. B. B.; Kim, H.; Ralph, J.; Martínez, Á. T.; del Río, J. C. Lignin composition and structure in young versus adult *Eucalyptus globulus* plants. *Plant Physiol.* **2011**, *155* (2), 667−682.

(8) Rencoret, J.; Kim, H.; Evaristo, A. B.; Gutiérrez, A.; Ralph, J.; del Río, J. C. Variability in lignin composition and structure in cell walls of different parts of macaúba (*Acrocomia aculeata*) palm fruit. *J. Agric. Food Chem.* **2018**, *66* (1), 138−153.

(9) del Río, J. C.; Rencoret, J.; Gutierrez, A.; Elder, T.; Kim, H.; Ralph, J. Lignin monomers from beyond the canonical monolignol biosynthetic pathway - Another brick in the wall. *ACS Sustainable Chem. Eng.* **2020**, *8*, 4997−5012.

(10) Lu, F.; Ralph, J. Preliminary evidence for sinapyl acetate as a lignin monomer in kenaf. *Chem. Commun.* **2002**, *2* (1), 90−91.

(11) del Río, J. C.; Marques, G.; Rencoret, J.; Martínez, Á. T.; Gutiérrez, A. Occurrence of naturally acetylated lignin units. *J. Agric. Food Chem.* **2007**, *55* (14), 5461.

(12) del Río, J. C.; Rencoret, J.; Marques, G.; Gutiérrez, A.; Ibarra, D.; Santos, J. I.; Jiménez-Barbero, J.; Zhang, L.; Martínez, Á. T. Highly acylated (acetylated and/or *p*-coumaroylated) native lignins from diverse herbaceous plants. *J. Agric. Food Chem.* **2008**, *56* (20), 9525.

(13) Martínez, A. T.; Rencoret, J.; Marques, G.; Gutiérrez, A.; Ibarra, D.; Jiménez-Barbero, J.; del Río, J. C. Monolignol acylation and lignin structure in some nonwoody plants: A 2D NMR study. *Phytochemistry* **2008**, *69* (16), 2831−2843.

(14) Rencoret, J.; Ralph, J.; Marques, G.; Gutiérrez, A.; Martínez, A. T.; del Río, J. C. Structural characterization of lignin isolated from coconut (*Cocos nucifera*) coir fibers. *J. Agric. Food Chem.* **2013**, *61* (10). 2434.

(15) Karlen, S. D.; Zhang, C.; Peck, M. L.; Smith, R. A.; Padmakshan, D.; Helmich, K. E.; Free, H. C. A.; Lee, S.; Smith, B. G.; Lu, F.; Sedbrook, J. C.; Sibout, R.; Grabber, J. H.; Runge, T. M.; Mysore, K. S.; Harris, P. J.; Bartley, L. E.; Ralph, J. Monolignol ferulate conjugates are naturally incorporated into plant lignins. *Sci. Adv.* **2016**, *2* (10), No. e1600393.

(16) Karlen, S. D.; Free, H. C. A.; Padmakshan, D.; Smith, B. G.; Ralph, J.; Harris, P. J. Commelinid monocotyledon lignins are acylated by *p*-coumarate. *Plant Physiol.* **2018**, *177* (2), 513−521.

(17) Kim, H.; Li, Q.; Karlen, S. D.; Smith, R. A.; Shi, R.; Liu, J.; Yang, C.; Tunlaya-Anukit, S.; Wang, J. P.; Chang, H.-M.; Sederoff, R. R.; Ralph, J.; Chiang, V. L. Monolignol benzoates incorporate into the lignin of transgenic *Populus trichocarpa* depleted in C3H and C4H. *ACS Sustainable Chem. Eng.* **2020**, *8*, 3644.

(18) del Río, J. C.; Prinsen, P.; Rencoret, J.; Nieto, L.; Jiménez-Barbero, J.; Ralph, J.; Martínez, Á. T.; Gutiérrez, A. Structural characterization of the lignin in the cortex and pith of elephant grass (*Pennisetum purpureum*) stems. *J. Agric. Food Chem.* **2012**, *60* (14), 3619−3634.

(19) Stewart, J. J.; Akiyama, T.; Chapple, C.; Ralph, J.; Mansfield, S. D. The effects on lignin structure of overexpression of ferulate 5-hydroxylase in hybrid poplar. *Plant Physiol.* **2009**, *150* (2), 621−635.

(20) Lu, F.; Karlen, S. D.; Regner, M.; Kim, H.; Ralph, S. A.; Sun, R. C.; Kuroda, K. i.; Augustin, M. A.; Mawson, R.; Sabarez, H.; Singh, T.; Jimenez-Monteon, G.; Zakaria, S.; Hill, S.; Harris, P. J.; Boerjan, W.; Wilkerson, C. G.; Mansfield, S. D.; Ralph, J. Naturally *p*-hydroxybenzoylated lignins in palms. *BioEnergy Res.* **2015**, *8* (3), 934−952.

(21) Lu, F.; Ralph, J. Novel *β*-*β*-structures in lignins incorporating acylated monolignols. *Appita Annu. Conf.* **2005**, *3*, 233−238.

(22) del Río, J. C.; Lino, A. G.; Colodette, J. L.; Lima, C. F.; Gutiérrez, A.; Martínez, Á. T.; Lu, F.; Ralph, J.; Rencoret, J. Differences in the chemical structure of the lignins from sugarcane bagasse and straw. *Biomass Bioenergy* **2015**, *81*, 322−338.

(23) Kaal, J.; Serrano, O.; Nierop, K. G. J.; Schellekens, J.; Martínez Cortizas, A.; Mateo, M. Á. Molecular composition of plant parts and sediment organic matter in a mediterranean seagrass (*Posidonia oceanica*) mat. *Aquat. Bot.* **2016**, *133*, 50−61.

(24) Kaal, J.; Serrano, O.; del Río, J. C.; Rencoret, J. Radically different lignin composition in *Posidonia* species may link to differences in organic carbon sequestration capacity. *Org. Geochem.* **2018**, *124*, 247−256.

(25) Tomlinson, P. B. On the morphology and anatomy of turtle grass, *Thalassia testudinum* (Hydrocharitaceae). III. Floral morphology and anatomy. *Bull. Mar. Sci.* **1969**, *19*, 286−305.
(26) Orth, R. J.; Carruthers, T. J. B.; Dennison, W. C.; Duarte, C. M.; Fourqurean, J. W.; Heck, K. L.; Hughes, A. R.; Kendrick, G. A.; Kenworthy, W. J.; Olyarnik, S.; Short, F. T.; Waycott, M.; Williams, S. L. A global crisis for seagrass ecosystems. *BioScience* **2006**, *56* (12), 987.
(27) Lu, F.; Ralph, J. Derivatization Followed by Reductive Cleavage (DFRC method), a new method for lignin analysis: Protocol for analysis of DFRC monomers. *J. Agric. Food Chem.* **1997**, *45* (7), 2590−2592.
(28) Balestri, E.; Vallerini, F.; Lardicci, C. A qualitative and quantitative assessment of the reproductive litter from *Posidonia oceanica* accumulated on a sand beach following a storm. *Estuarine, Coastal Shelf Sci.* **2006**, *66* (1−2), 30−34.
(29) Fornes, A.; Basterretxea, G.; Orfila, A.; Jordi, A.; Alvarez, A.; Tintore, J. Mapping *Posidonia oceanica* from IKONOS. *ISPRS J. Photogramm. Remote Sens.* **2006**, *60* (5), 315−322.
(30) Parry, E. Beachcomber's treasure — a sea ball. *Nat. Hist.* **1956**, *65*, 496−497.
(31) Tappi. *Tappi Test Methods 2004−2005*; Tappi Press: Norcoss, GA, 2004.
(32) Björkman, A. Isolation of lignin from finely divided wood with neutral solvents. *Nature* **1954**, *174*, 1057−1058.
(33) Rencoret, J.; Neiva, D.; Marques, G.; Gutiérrez, A.; Kim, H.; Gominho, J.; Pereira, H.; Ralph, J.; del Río, J. C. Hydroxystilbene glucosides are incorporated into Norway spruce bark lignin. *Plant Physiol.* **2019**, *180* (3), 1310−1321.
(34) Ralph, J.; Hatfield, R. D. Pyrolysis-GC-MS Characterization of forage materials. *J. Agric. Food Chem.* **1991**, *39* (8), 1426−1437.
(35) Ralph, J.; Lu, F. The DFRC method for lignin analysis. 6. A simple modification for identifying natural acetates on lignins. *J. Agric. Food Chem.* **1998**, *46* (11), 4616−4619.
(36) del Río, J. C.; Rencoret, J.; Prinsen, P.; Martínez, Á. T.; Ralph, J.; Gutiérrez, A. Structural characterization of wheat straw lignin as revealed by analytical pyrolysis, 2D-NMR, and reductive cleavage methods. *J. Agric. Food Chem.* **2012**, *60* (23), 5922−5935.
(37) del Río, J. C.; Rencoret, J.; Gutiérrez, A.; Kim, H.; Ralph, J. Hydroxystilbenes are monomers in palm fruit endocarp lignins. *Plant Physiol.* **2017**, *174* (4), 2072−2082.
(38) Zinovyev, G.; Sumerskii, I.; Rosenau, T.; Balakshin, M.; Potthast, A. Ball milling's effect on pine milled wood lignin's structure and molar mass. *Molecules* **2018**, *23* (9), 2223.
(39) del Río, J. C.; Martin, F.; Gonzalez-Vila, F. J. Thermally assisted hydrolysis and alkylation as a novel pyrolytic approach for the structural characterization of natural biopolymers and geomacromolecules. *Trends Anal. Chem.* **1996**, *15* (2), 70−79.
(40) Ohtani, H.; Fujii, R.; Tsuge, S. Pyrolysis - capillary gas chromatography combined with on-line alkylation for the compositional analysis of liquid crystalline aromatic polyesters. *J. High Resolut. Chromatogr.* **1991**, *14* (6), 388−391.
(41) Kuroda, K. I.; Ozawa, T.; Ueno, T. Characterization of sago palm (*Metroxylon sagu*) lignin by analytical pyrolysis. *J. Agric. Food Chem.* **2001**, *49* (4), 1840−1847.
(42) Mackay, H. A. Identifying a native *p*-hydroxybenzoyl-CoA monolignol transferase gene in poplar. Ph.D. Thesis, University of British Columbia, 2019. DOI: 10.14288/1.0380258.
(43) Lan, W.; Rencoret, J.; Lu, F.; Karlen, S. D.; Smith, B. G.; Harris, P. J.; del Río, J. C.; Ralph, J. Tricin-lignins: Occurrence and quantitation of tricin in relation to phylogeny. *Plant J.* **2016**, *88* (6), 1046.
(44) Ralph, J.; Hatfield, R. D.; Quideau, S.; Helm, R. F.; Grabber, J. H.; Jung, H. J. G. Pathway of *p*-coumaric acid incorporation into maize lignin as revealed by NMR. *J. Am. Chem. Soc.* **1994**, *116* (21), 9448−9456.
(45) Rencoret, J.; Prinsen, P.; Gutiérrez, A.; Martínez, Á. T.; del Río, J. C. Isolation and structural characterization of the milled wood lignin, dioxane lignin, and cellulolytic lignin preparations from brewer's spent grain. *J. Agric. Food Chem.* **2015**, *63* (2), 603−613.
(46) Lu, F.; Ralph, J. DFRC method for lignin analysis. 1. New method for *β*-aryl ether cleavage: Lignin model studies. *J. Agric. Food Chem.* **1997**, *45* (12), 4655−4660.
(47) Karlen, S. D.; Smith, R. A.; Kim, H.; Padmakshan, D.; Bartuce, A.; Mobley, J. K.; Free, H. C. A.; Smith, B. G.; Harris, P. J.; Ralph, J. Highly decorated lignins in leaf tissues of the Canary Island date palm *Phoenix canariensis*. *Plant Physiol.* **2017**, *175* (3), 1058−1067.
(48) Bitam, F.; Ciavatta, M. L.; Manzo, E.; Villani, G.; Gavagnin, M. The first record of neolignans from the marine phanerogam *Posidonia oceanica*. *Phytochem. Lett.* **2012**, *5* (4), 696−699.
(49) Ralph, J.; Karlen, S.; Mobley, J. Synthesis of paracetamol (acetaminophen) from biomass-derived *p*-hydroxybenzamide. Patent US10286504B2, 2019.